

LLNL LASER-COMPTON X-RAY CHARACTERIZATION*

Y. Hwang[†], T. Tajima, University of California, Irvine, CA USA 92697
 G. Anderson, D. J. Gibson, R. A. Marsh, C. P. J. Barty,
 Lawrence Livermore National Laboratory, Livermore, CA USA 94550

Abstract

30 keV Compton-scattered X-rays have been produced at LLNL. The flux, bandwidth, and X-ray source focal spot size have been characterized using an X-ray ICCD camera and results agree very well with modeling predictions. The RMS source size inferred from direct electron beam spot size measurement is $17\ \mu\text{m}$, while imaging of the penumbra yields an upper bound of $42\ \mu\text{m}$. The accuracy of the latter method is limited by the spatial resolution of the imaging system, which has been characterized as well, and is expected to improve after the upgrade of the X-ray camera later this year.

INTRODUCTION

X-ray and γ -ray generation by laser-Compton scattering (LCS) is being studied worldwide for its potential as a compact synchrotron quality X-ray source [1–5]. At LLNL, an X-band linac has been built and is in operation to produce laser-Compton scattered X-rays [6]. Important features including flux and bandwidth of the X-rays have been characterized using an X-ray CCD camera and simulations [7]. X-ray flux was measured with a calibrated camera and matched the value expected from simulations.

For bandwidth demonstration, a $50\ \mu\text{m}$ silver foil was placed in front of the camera and the beam energy was tuned to produce X-rays with peak energy just above the K absorption edge of silver (25.5 keV). Due to Doppler shifting, X-ray energy decreases as observance angle deviates from the axis of the electron beam. This energy-angle correlation creates a dark disc in the center where the X-ray energy is above the K-edge and therefore highly attenuated, surrounded by a bright background where energy is below the K-edge. The steepness of contrast is directly related to the bandwidth of the X-rays, and simulation was able to reproduce the image extremely well with expected parameters, as shown in Figure 1.

Small X-ray source size is a characteristic of Compton light sources that is of particular importance in several imaging applications such as phase contrast imaging [8], but accurate source size measurement has yet to be achieved due to the limited imaging capability of the current setup.

* This work performed under the auspices of the U.S. Department of Energy by Lawrence Livermore National Laboratory under Contract DE-AC52-07NA27344.

[†] yoonwooh@uci.edu

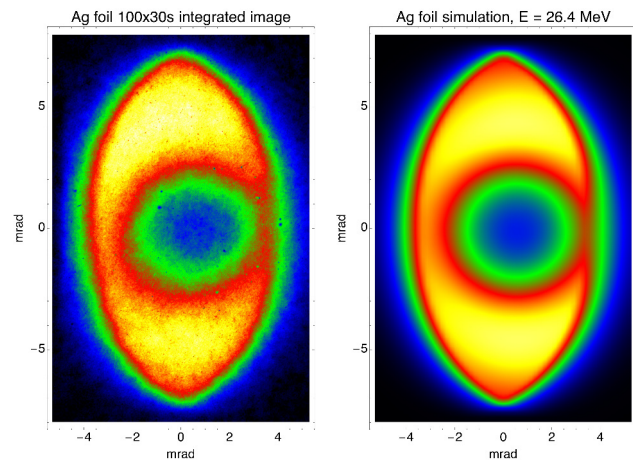


Figure 1: 3,000 second integration image of $50\ \mu\text{m}$ Ag foil K-edge hole (left) and its simulation (right).

SPATIAL RESOLUTION AND SOURCE SIZE

The spatial resolution of a radiograph depends strongly on both the source size and the imaging system's resolving power. The source size of our X-ray beam is similar to the size of the electron spot size at the interaction point, since the electron spot size is smaller than the laser spot size. The RMS source focal spot size σ_s can be defined from the geometric unsharpness formula $\sigma_s = \sigma_p a/b$, where σ_p is the RMS penumbra size, a is the source to object distance and b is the object to detector distance. Modeling of radiographs using the image simulation code described in [7] shows excellent agreement of the above-defined source size and the electron beam spot size.

Single shot OTR images of the electron beam spot at the interaction point show an RMS size of $14\ \mu\text{m}$ in horizontal and $11\ \mu\text{m}$ in vertical, with jitter around $5\ \mu\text{m}$ by $3\ \mu\text{m}$ [9]. The integrated image of 1,000 overlapped shots (Figure 2) yields $16.7\ \mu\text{m}$ by $12.8\ \mu\text{m}$ and is very close to Gaussian in profile (Figure 3).

Therefore, in order to measure the penumbra and the X-ray source size directly, a very high resolution imaging device is necessary; otherwise the blur from the imaging system will dominate the resolution of the result, rendering source size determination impossible. The large field-of-view Andor X-ray CCD camera that was used to characterize the beam's flux and bandwidth is not capable of resolving small details necessary for the source size measurement, due to scintillator thickness, 3:1 demagnification fiber optic taper and multiple fiber optic relays, in addition to dimmed and non-uniform

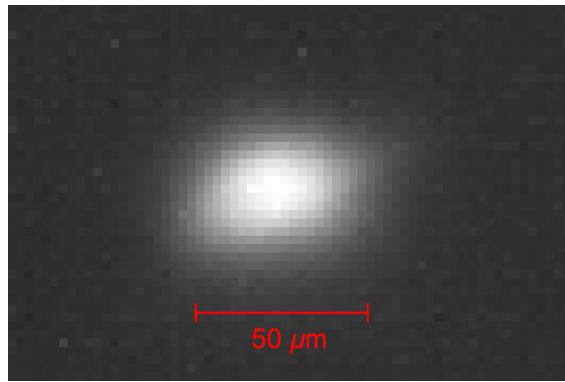


Figure 2: 1,000 shot OTR image of the electron beam at the interaction point.

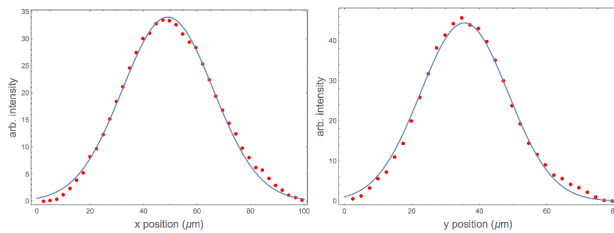


Figure 3: Integrated lineout profiles in red and their Gaussian fits in blue in the horizontal (left) and vertical (right) directions of Figure 2.

sensitivity of the CCD owing to extensive radiation damage from previous Compton scattered γ -ray experiments [10]. The spatial resolution of the camera measured with a sharp edge varied between $350\ \mu\text{m}$ and $700\ \mu\text{m}$ FWHM depending on the scintillation material used. We have purchased a new CCD camera with a thin scintillator and lens relay system allowing $11\ \mu\text{m}$ spatial resolution from Crytur, which is expected to be delivered shortly. Meanwhile, we have characterized the beam using another Andor camera identical to our current camera in a slightly different setup, with a $150\ \mu\text{m}$ CsI scintillator and without the 3:1 taper. The pixel size is $13\ \mu\text{m}$ with field of view of 13 by 13 mm.

MEASUREMENT OF SPATIAL RESOLUTION OF THE IMAGING SYSTEM

To measure the resolution of the camera, a wedge-type line pair gauge etched from $30\ \mu\text{m}$ thick Pb was placed directly in front of the scintillator. This eliminates the penumbra from the source, and the sharp edges of the resolution test pattern are blurred solely due to the imaging system. Figure 4 shows the resulting image captured by summing 100 30 s exposure images, for a total exposure time of 50 minutes. Sample lineout profiles at $6.9\ \text{lp/mm}$ and $10.4\ \text{lp/mm}$ is shown in Figure 5.

A fit of the lineout was made by convolving a square wave function of appropriate frequency representing the line pairs with a Cauchy distribution of varying FWHM. Image blur-

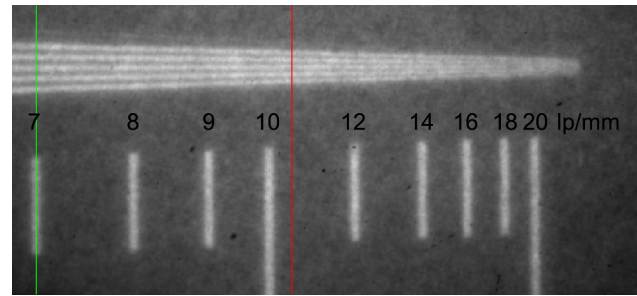


Figure 4: 50 minute integration image of the resolution test pattern at unity magnification.

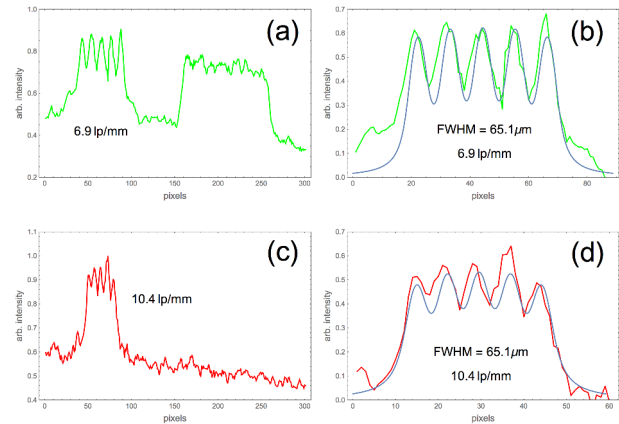


Figure 5: Lineout profiles of Figure 4 (a,c) and their Cauchy distribution convolution fit in blue (b,d).

ring in the scintillator is a result of X-ray photons creating electron-hole pairs which then travel along the crystal as they migrate to impurity centers where energy is given off as visible light [11], and therefore the point spread function is highly peaked with long tails, justifying the use of Cauchy distribution as the fitting function. A blur of $65\ \mu\text{m}$ FWHM Cauchy distribution was found to fit the data well across most frequencies; this is regarded as the upper bound since the resolution could be smaller if signal to noise was better.

MEASUREMENT OF SOURCE SIZE

For the source size measurement, the line pair gauge was placed as close as possible to the X-ray source (laser-Compton interaction point) to create maximum magnification and penumbra. The image was magnified $1.7\times$, and the corresponding imaging simulation showed that the blurs in line pair images at this distance can be well approximated by a Gaussian blur with $\sigma = 0.7\sigma_e$, where σ_e is the RMS width of the electron beam. Hence, the fit was made by convolving square wave functions with a Gaussian distribution kernel, then further convolving it with a $65\ \mu\text{m}$ FWHM Cauchy distribution kernel. The resulting image and the fits of two sample lineouts are shown in Figures 6 and 7 respectively. The image was acquired by summing 75 1-minute integration images, for a total exposure time of 75 minutes.

The upper bound for Gaussian σ in the fit was $30\ \mu\text{m}$, corresponding to a maximum source size (and electron beam

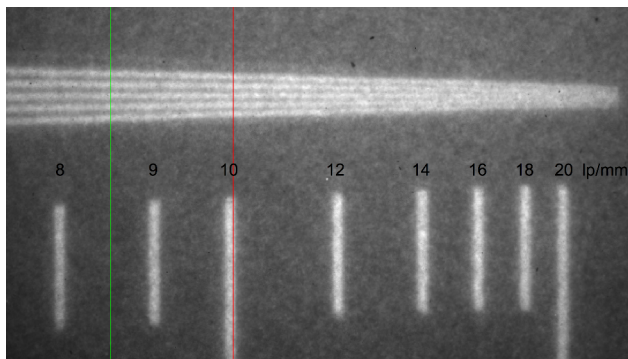


Figure 6: 75 minute integration image of the resolution test pattern at 1.7x magnification.

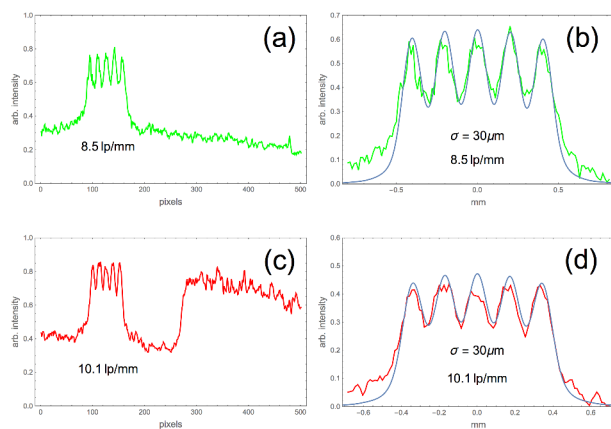


Figure 7: Lineout profiles of Figure 6 (a,c) and their Gaussian+Cauchy distribution convolution fit in blue (b,d).

size) of $42 \mu\text{m}$ RMS, or $100 \mu\text{m}$ FWHM. This upper bound value is much higher than the measured electron beam size due to limitations in the imaging system; the scintillator blur is of comparable size and the signal-to-noise ratio is low as evidenced by the image. The new Crytur camera with claimed $11 \mu\text{m}$ spatial resolution will dramatically improve the accuracy and bring the value down closer to the measured electron beam size.

CONCLUSION

X-rays produced from the Laser-Compton X-ray source at LLNL have been thoroughly characterized; the flux and bandwidth match well with simulation results. Advancements in direct measurement of the source size has been made through a new camera setup and modeling analysis despite the limited resolution of the imaging system. There is still much room for improvement; a new high-resolution X-ray camera is on order and is expected to arrive within this year.

REFERENCES

- [1] I. V. Pogorelsky *et al.*, "Demonstration of 8×10^{18} photons/second peaked at 1.8 \AA in a relativistic Thomson scattering experiment," *Phys. Rev. ST Accel. Beams*, vol. 3, p. 090702, 2000.
- [2] R. Kuroda *et al.*, "Quasi-monochromatic hard X-ray source via laser Compton scattering and its application," *Nucl. Instr. Meth. A*, vol. 637, pp. S183-S186, 2011.
- [3] Y. Du *et al.*, "Generation of first hard X-ray pulse at Tsinghua Thomson Scattering X-ray Source," *Rev. Sci. Instr.*, vol. 84, p. 053301, 2013.
- [4] Y. K. Wu, "Accelerator physics research and light source development at Duke University," in *Proc. IPAC'10*, Kyoto, Japan, May 2010, paper WEPEA071, pp. 2648–2650.
- [5] R. J. Loewen, "A compact light source: Design and technical feasibility study of a laser-electron storage ring X-ray source," Stanford Linear Accelerator Center, Stanford University, Stanford, CA, USA, 2003.
- [6] D. J. Gibson *et al.*, "Multi-GHz pulse-train X-band capability for laser Compton X-ray and γ -ray sources," in *Proc. IPAC'15*, Richmond, VA, USA, May 2015, paper TUBC2, pp. 1363–1365.
- [7] Y. Hwang *et al.*, "LLNL laser-Compton X-ray characterization," in *Proc. IPAC'16*, Busan, Korea, May 2016, paper TUPOW052, pp. 1885–1888.
- [8] Alberto Bravin *et al.*, "X-ray phase-contrast imaging: from pre-clinical applications towards clinics," *Phys. Med. Biol.* vol. 58, pp. R1-R35, 2013.
- [9] R. A. Marsh *et al.*, "LLNL X-band RF gun results," in *Proc. IPAC'16*, Busan, Korea, May 2016, paper THPOW026, pp. 3993–3995.
- [10] F. Albert *et al.*, "Characterization and applications of a tunable, laser-based, MeV-class Compton-scattering γ -ray source," *Phys. Rev. ST Accel. Beams*, vol. 13, p. 070704, 2010.
- [11] Martin Mikl, "Scintillation detectors for x-rays," *Meas. Sci. Technol.*, vol. 17, pp. R37-R54, 2006.